Slow relaxation of the magnetization on frustrated triangular Fe^{III} units with S = 1/2 ground state: the effect of the highly ordered crystal lattice and the counter-anions.

Walter Cañón-Mancisidor[a,b,d]*, Patricio Hermosilla-Ibáñez[b,c], Evgenia Spodine[b,d]*, Verónica Paredes-García[b,e], Carlos J. Gómez-García[f], Guillermo Mínguez Espallargas[f], Diego Venegas-Yazigi[b,c]*.

[a] *Depto. Matemáticas y Ciencias de la Ingeniería (DMCI), Facultad de Ingeniería, Ciencia y tecnología (FICyT), Universidad Bernardo O'Higgins (UBO), Av. Viel 1497, Santiago, CP-8370993, Chile.*

[b] *Centro para el Desarrollo de la Nanociencia y Nanotecnología, (CEDENNA), USACH, Av. Lib Bernardo O´Higgins 3363, Estación Central, CP-9170022, Chile.*

[c] *Depto. Química de los Materiales, Facultad de Química y Biología, Universidad de Santiago de Chile (USACH), Av. Lib Bernardo O´Higgins 3363, Estación Central, CP-9170022, Chile.*

[d] *Facultad de Ciencias Químicas y Farmacéuticas, Universidad de Chile, Dr. Carlos Lorca Tobar 964, Independencia, CP-8380000 Chile.*

[e] *Departamento de Ciencias Químicas, Universidad Andrés Bello (UNAB), República 276, Santiago, CP-8370134, Chile.*

[f] *Instituto de Ciencia Molecular (ICMol), Universidad de Valencia, C/ Catedrático Jose Beltrán, 2, 46980 Paterna, Valencia, Spain.*

*E-mail: : walter.canon@ubo.cl, diego.venegas@usach.cl and espodine@uchile.cl.

KEYWORDS Triangular complexes, molecular magnetism, Fe^{III} complexes, Slow relaxation.

ABSTRACT: In order to understand how the different arrangements of highly ordered triangular Fe^{III} S = 1/2 systems with various types of diamagnetic and paramagnetic anions affect their static and dynamic magnetic properties, we have obtained by solvothermal synthesis four new μ_3-oxido trinuclear Fe^{III} compounds, $[Fe_3O(Ac)_6(AcNH_2)_3][BF_4]\cdot(CH_3CONH_2)_{0.5}(H_2O)_{0.5}$ (**1-BF_4**), $[Fe_3O(Ac)_6(AcNH_2)_3][GaCl_4]$ (**1-$GaCl_4$**), $[Fe_3O(Ac)_6(AcNH_2)_3][FeCl_4]$ (**1-$FeCl_4$**) and $[Fe_3O(Ac)_6(AcNH_2)_3][FeBr_4]$ (**1-$FeBr_4$**), where, $Ac^- = CH_3COO^-$ and $AcNH_2 = CH_3CONH_2$. The organization of the triangular units is very varied, from segregated stacks to eclipsed equilateral triangular $[Fe_3O]^+$ units along the *c* axis with intercalated $[MX_4]^-$ units. The ordering of the triangular species together with disposition of the counter-anions (intercalated or not) affects the static and dynamic magnetic properties of the $[Fe_3O]^+$ systems. Magnetic *dc* data were satisfactorily fitted with a HDvV spin Hamiltonian also considering the existence of anisotropic phenomena (antisymmetric exchange and intermolecular interactions), in order to model the low temperature region. From the antisymmetric exchange, we were able to obtain Δ (U_{eff}), which was used to model and rationalize the dynamic magnetic properties of these systems, reflecting that Orbach and Raman processes define the relaxation mechanism of these systems.

INTRODUCTION

Triangular complexes are an interesting class of materials since they have been suggested as possible qubits, due to the spin-electron coupling as a result of the interplay between the spin exchange, spin-orbit interaction and the chirality of the spin system of the molecule.[1,2] These features are due to the existence of spin frustration phenomena, which originates in a system with an odd number of non-integer spins that are antiferromagnetically coupled, since the spin carriers cannot be satisfied simultaneously.[3] This causes, from the energy point of view, a ground state that is doubly degenerated. This degeneracy can be broken by lowering the symmetry of the systems due to distortions of the C_3 symmetry of the triangle or by the antisymmetric exchange, which is related to spin-orbit interactions.[4,5]

From a magnetic point of view, $[M_3O(RCOO)_6L_3]^+$ compounds have been used as models to study the magnetic and electronic interaction between the metal centers on polynuclear complexes.[6–9] The electronic structure of these trinuclear μ_3-oxido transition metal complexes has been the subject of extensive studies over many years.[10–15] One of the most studied species, known as "basic carboxylates", are the trinuclear oxido centered iron(III) complexes.[16–18] Actually, these systems were neglected for many years, but the novel studies done by Boudalis et al.[19,20] have shown many interesting magnetic properties, allowing to define these systems as spin-triangle molecular qubits, showing spin decoherence and making these compounds relevant for quantum computing.[21]

The $[Fe_3O]^+$ core can be found as equilateral, isosceles or scalene triangles, being the geometry, spin-orbit interactions and the type of the paramagnetic counter-anion, the main factors affecting the overall magnetic behavior of these system.[4,5] Thus, species like the anion $[MX_4]^-$,[27–36] much less common than other anions such as ClO_4^-,[4,22] NO_3^- [23,24] or Cl^-, [25,26] can affect the intramolecular magnetic interactions, as well as the intermolecular ones.

In order to understand the role of the crystalline ordering (the way that cations and anions arrange in the crystalline lattice) of triangular $[Fe_3O]^+$ S = 1/2 units and their counter-anions

Table 1. Crystal and structure refinement data for $[Fe_3O(Ac)_6(AcNH_2)_3][BF_4]$ **(1-BF$_4$)**, $[Fe_3O(Ac)_6(AcNH_2)_3][GaCl_4]$ **(1-GaCl$_4$)**, $[Fe_3O(Ac)_6(AcNH_2)_3][FeCl_4]$ **(1-FeCl$_4$)** and $[Fe_3O(Ac)_6(AcNH_2)_3][FeBr_4]$ **(1-FeBr$_4$)**.

Compound	1-BF$_4$	1-GaCl$_4$	1-FeCl$_4$	1-FeBr$_4$
Formula weight	840.4	926.5	912.7	1090.5
Temperature	120 K	120 K	120 K	120 K
Wavelength	Mo, 0.71073 Å	Mo, 0.71073 Å	Mo, 0.71073 Å	Mo, 0.71073 Å
Crystal System, Space group	Monoclinic, $P2_1/n$	Trigonal, $R\bar{3}$	Trigonal, $R\bar{3}$	Trigonal, $R\bar{3}$
Unit cell dimensions	a = 8.0519(8) Å b = 26.236(2) Å c = 17.0781(13) Å α = 90° β = 92.556(8)° γ = 90°	$a = b$ = 15.6365(6) Å c = 12.8586(7) Å α = 90° β = 90° γ = 120°	$a = b$ = 15.3756(2) Å c = 12.8829(3) Å α = 90° β = 90° γ = 120°	$a = b$ = 15.9870(4) Å c = 12.9357(6) Å α = 90° β = 90° γ = 120°
Volume	3604.1(5) Å^3	2722.7(3) Å^3	2637.60(9) Å^3	2863.2(2) Å^3
Z	2	3	3	3
Absorption coefficient	1.281 mm^{-1}	2.269 mm^{-1}	1.988 mm^{-1}	5.738 mm^{-1}
Color	red	red	red	red
Limiting indices	-10 ≤ h ≤ 10 -34 ≤ k ≤ 34 -22 ≤ l ≤ 21	-19 ≤ h ≤ 19 -19 ≤ k ≤ 19 -16 ≤ l ≤ 16	-18 ≤ h ≤ 18 -18 ≤ k ≤ 18 -15 ≤ l ≤ 15	-20 ≤ h ≤ 20 -20 ≤ k ≤ 20 -16 ≤ l ≤ 16
Reflections collected, unique	39112,8286	10380, 2485	12617, 2083	10518, 2941
Refinement method	Full-matrix least squares on F^2	Full-matrix least squares on F^2	Full-matrix least squares on F^2	Full-matrix least squares on F^2
Data / parameters	8286 / 498	2485 / 177	2083 / 140	2941 / 139
Goodness-of-fit on F^2	1.029	1.054	1.194	1.153
Final R indexes [I>2sigma(I)]	Rf = 0.0746, wR = 0.1722	Rf = 0.0378, wR = 0.0832	Rf = 0.0500, wR = 0.1201	Rf = 0.0453, wR = 0.1166
Largest diff. peak/hole / e Å^{-3}	1.46/-1.07	0.45/-0.66	0.55/-0.65	0.57/-1.52
Flack parameter		-0.001(9)	0.06(6)	0.025(26)

(paramagnetic and diamagnetic) on the static and dynamic magnetic properties, we herein report the structural characterization and magnetic studies of four new μ$_3$-oxido trinuclear Fe^{III} compounds, $[Fe_3O(Ac)_6(AcNH_2)_3][BF_4]\cdot(CH_3CONH_2)_{0.5}(H_2O)_{0.5}$ (**1-BF$_4$**), $[Fe_3O(Ac)_6(AcNH_2)_3][GaCl_4]$ (**1-GaCl$_4$**), $[Fe_3O(Ac)_6(AcNH_2)_3][FeCl_4]$ (**1-FeCl$_4$**) and $[Fe_3O(Ac)_6(AcNH_2)_3][FeBr_4]$ (**1-FeBr$_4$**). The results show that both, *dc* and *ac* magnetic properties can be affected by the ordering of the triangular units, as well as by the type of counter-anions present in the crystal lattice.

EXPERIMENTAL

Synthesis

$[Fe_3O(Ac)_6(AcNH_2)_3][BF_4]\cdot(CH_3CONH_2)_{0.5}(H_2O)_{0.5}$ (1-BF$_4$). $Fe(BF_4)_2\cdot 6H_2O$ (1013 mg, 3 mmol), triethanolamine hydrochloride (185 mg, 1 mmol) and sodium acetate trihydrate (408 mg, 3 mmol) were mixed in 5 mL of CH_3CN in a Parr reactor and heated under autogenous pressure at 150 °C for 48 hours. The reaction mixture was filtered off and red crystals suitable for X-ray diffraction were obtained within three days by slow evaporation of the mother liquor at room temperature.

Elemental analysis for **1-BF$_4$**: Found: C, 26.8; N, 5.3; H, 4.1 %. Calc. for $Fe_3C_{19}H_{36.5}N_{3.5}O_{17}BF_4$: C, 27.2; N, 5.8; H, 4.3 %. IR data (KBr, ν_{max}/cm^{-1}) 3432w and 3355m [ν(NH amide)], 1666w [ν_{as}(COO)], 1444w [ν_s(COO)] and 615m [ν_{as}(Fe_3O)] (Table S1).

$[Fe_3O(Ac)_6(AcNH_2)_3][GaCl_4]$ (1-GaCl$_4$). $FeCl_3\cdot 6H_2O$ (810 mg, 3 mmol), $Ga(NO_3)_3\cdot 6H_2O$ (383 mg, 1 mmol), triethanolamine hydrochloride (185 mg, 1 mmol) and sodium acetate trihydrate (408 mg, 3 mmol) were mixed in 5 mL of CH_3CN in a Parr reactor and heated under autogenous pressure at 150 °C for 48 hours. Dark red crystals of **1-GaCl$_4$** suitable for X-ray diffraction were obtained after three days by slow evaporation of the mother liquor at room temperature.

Elemental analysis for **1-GaCl$_4$**: Found: C, 23.0 %; N, 5.2 %; H, 4.3 %. Calc. for $Fe_3Ga_1C_{18}H_{33}N_3O_{16}Cl_4$: C, 23.3 %; N, 4.5 %; H, 3.6 %. IR data (KBr, ν_{max}/cm^{-1}) 3423w and 3353m [ν(NH amide)], 1660w [ν_{as}(COO)], 1444w [ν_s(COO)], 614m [ν_{as}(Fe_3O)], (Table S1).

Mass-spectrometry confirms the existence only of Fe_3O cationic units in **1-GaCl$_4$** and no pattern for Fe_2GaO, $FeGa_2O$ or Ga_3O cationic units were detected. (Figure S1). The experiments show the presence of $[Fe_3O(Ac)_6]^+$ (m/Z = 538); $[Fe_3O(Ac)_6\text{-}CH_3CN]^+$ (m/Z = 579); $[Fe_3O(Ac)_6(CH_3CONH_2)]^+$ (m/Z = 597) and $[Fe_3O(Ac)_6(CH_3CONH_2)_2]^+$ (m/Z = 656) units. The elemental Ga:Fe ratio, estimated by electron probe microanalysis (EPMA), is 1.00:3.03. (Calculated Ga:Fe = 1.00:3.00).

$[Fe_3O(Ac)_6(AcNH_2)_3][FeX_4]$ with X = Cl (1-FeCl$_4$) and Br (1-FeBr$_4$). The corresponding Fe^{III} halides (3 mmol of $FeCl_3\cdot 6H_2O$ (810 mg) for **1-FeCl$_4$** and $FeBr_3$ (870 mg) for **1-FeBr$_4$**), triethanolamine hydrochloride (185 mg, 1 mmol) and sodium acetate trihydrate (408 mg, 3 mmol) were mixed in 5 mL of acetonitrile (CH_3CN) in a Parr reactor and heated under autogenous pressure at 150 °C for 48 hours. The reaction mixture was filtered off and dark red crystals of both compounds suitable for X-ray diffraction were obtained within three days by slow evaporation of the mother liquors at room temperature.

Elemental analysis for **1-FeCl$_4$**: Found: C, 24.1 %; N, 4.7 %; H, 3.7 %. Calc. for $Fe_4C_{18}H_{33}N_3O_{16}Cl_4$: C, 23.7 %; N, 4.6 %; H, 3.6 %). IR data (KBr, ν_{max}/cm^{-1}) 3424w and 3349m [ν(NH amide)], 1658w, [ν_{as}(COO)] 1444w [ν_s(COO)] and 613m [ν_{as}(Fe_3O)] (Table S1).

Elemental analysis for **1-FeBr$_4$**: Found: C,20.2 %; N, 4.1 %; H, 3.2 %. Calc. for $Fe_4C_{18}H_{33}N_3O_{16}Br_4$: C, 19.8 %; N, 3.9 %; H, 3.0 %. IR data (KBr, ν_{max}/cm^{-1}) 3421w and 3353m [ν(NH amide)], 1662w, [ν_{as}(COO)], 1444w [ν_s(COO)] and 611m [ν_{as}(Fe_3O)] (Table S1).

Compound Physical Characterization

Fourier transform infrared spectroscopy (FTIR) was performed using a NICOLET 5700 in the range of 4000 to 650 cm^{-1} for the crystalline materials. Elemental analysis (C, N, H) of

bulk samples was performed by microanalytical procedures using a CE Instruments ED 1108. *Electrospray ionization mass spectrometry* (ESI-MS) studies were done on compound **1-GaCl$_4$** with a QTOF Premier instrument with an orthogonal Z-spray-electrospray interface (Waters, Manchester, UK). A capillary voltage of 3.5 kV was used in the positive scan mode and the cone voltage set to 10 V to control the extent of fragmentation. *mMass* code was used to simulate the isotopic pattern of the molecule. The Fe: Ga ratio of the bulk samples of **1-GaCl$_4$** were estimated by *electron probe microanalysis* EPMA), performed with a Philips SEM XL30 equipped with an EDAX DX-4 microprobe.

X-Ray Diffraction

Single crystals of all compounds were mounted on glass fibres, using a viscous hydrocarbon oil to coat the crystal, and then transferred directly to the cold nitrogen stream for data collection. X-ray data were collected at 120 K on a Supernova diffractometer equipped with a graphite-monochromated Enhance (Mo) X-ray Source (λ = 0.71073 Å) and on a Bruker Smart APEX2 diffractometer. Data sets were reduced by using SAINT,[27] while the structures were solved by direct methods and completed by difference Fourier synthesis. Least-squares refinement was conducted by using SHELXL.[28,29]

Non-hydrogen atoms were refined anisotropically (except the disordered fragments) and hydrogen atoms were placed in calculated positions that were refined using idealized geometries (riding model) and assigned fixed isotropic displacement parameters except for those of water molecules, which were located and refined with distance restraints. In **1-BF$_4$** the H_2O and $AcNH_2$ solvation molecules are disordered over two sites and were modelled with a 0.339:0.661 ratio. Structural drawings were carried out with DIAMOND-3.2k, supplied by Crystal Impact.[30] A summary of the data collection and structure refinements is provided in Table 1. The CCDC codes 1547609 **(1-BF$_4$)**, 1547610 **(1-GaCl$_4$)**, 1547607 **(1-FeCl$_4$)** and 1547608 **(1-FeBr$_4$)** contain the supplementary crystallographic data for this paper. These data can be obtained free of charge from The Cambridge Crystallographic Data Centre via www.ccdc.cam.ac.uk/data_request/cif.

Magnetic Susceptibility Measurements

Variable temperature *dc* susceptibility measurements were carried out for all compounds on ground polycrystalline samples (with masses of 12.00, 14.87, 16.47 and 15.95 mg for **1-BF$_4$**, **1-GaCl$_4$**, **1-FeCl$_4$** and **1-FeBr$_4$**, respectively) in the temperature range 2-300 K with an applied magnetic field of 1000 G. The measurements were done with a MPMS-XL-5 SQUID susceptometer and a PPMS DynaCool^{TM} (Quantum Design). The susceptibility data were corrected for the diamagnetic contributions of the sample, using Pascal´s constants.[31] Isothermal magnetization measurements were made between 0 and 5 T at different temperatures. Variable temperature *ac* magnetization measurements were performed in a PPMS DynaCool^{TM} systems (Quantum Design) with an alternating field of 3 to 10 G, at frequencies in the range 10-10000 Hz in the temperature range 2-

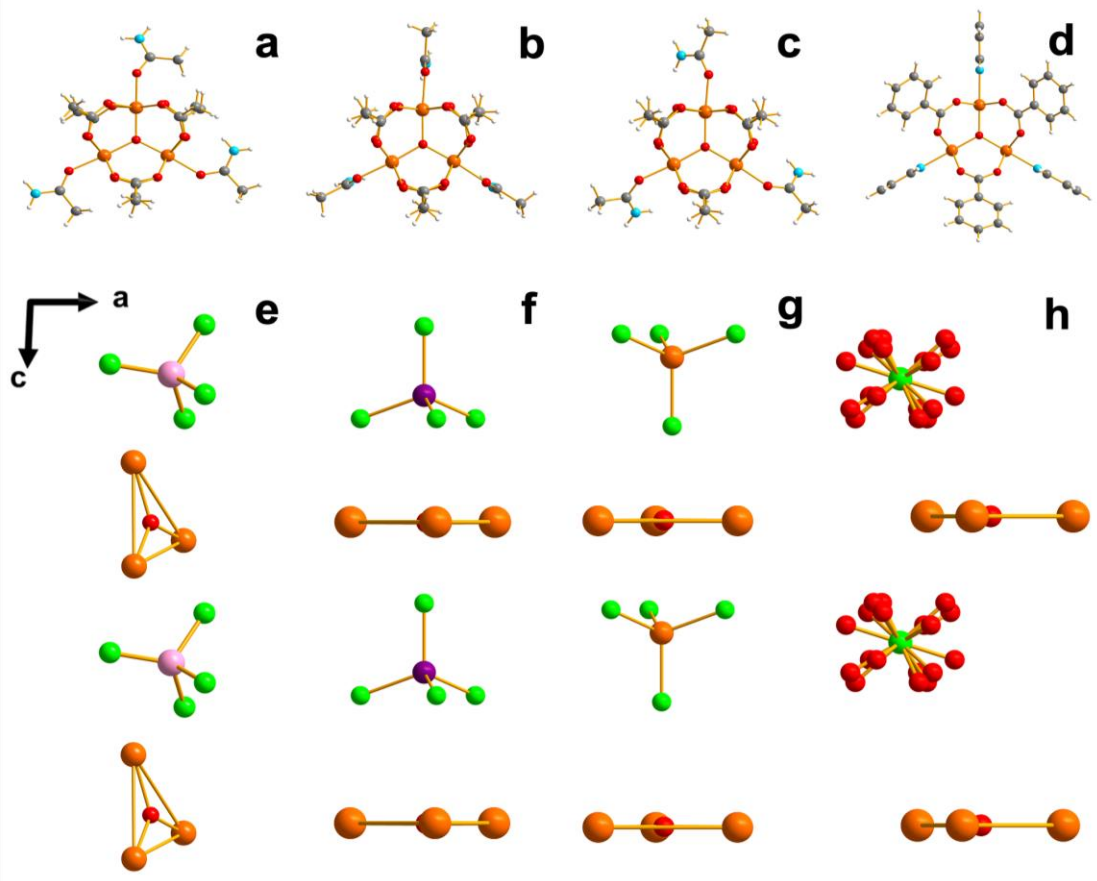

Figure 1. (**a-d**) Triangular units of complexes $[Fe_3O(Ac)_6(AcNH_2)_3][BF_4]$ **(1-BF$_4$)**, $[Fe_3O(Ac)_6(AcNH_2)_3][GaCl_4]$ **(1-GaCl$_4$)**, $[Fe_3O(Ac)_6(AcNH_2)_3][FeCl_4]$ **(1-FeCl$_4$)** and $[Fe_3O(Ac)_6(AcNH_2)_3][ClO_4]$ **(QOPLUC).** (**e-h**). Representation of the crystal lattice arrangements of cationic triangular units and the counter-anion of the complexes. Color code: Fe = orange, O = red, N = light blue, C = grey, H = white.

10 K and with three different *dc* magnetic fields (3000, 5000 and 7000 G).

RESULTS AND DISCUSSION

Synthesis

Although acetamide ($AcNH_2$) is not included as starting reagent, all compounds present acetamide ligands in their structure, which originates from the hydrolysis of acetonitrile under solvothermal conditions, as previously reported.[32]

Structural Analysis

Compounds **1-BF$_4$**, **1-GaCl$_4$,** **1-FeCl$_4$** and **1-FeBr$_4$** are formed by the cationic complex $[Fe_3O(Ac)_6(AcNH_2)_3]^+$ (Figure 1), whose charge is counterbalanced by the anions $[BF_4]^-$, $[GaCl_4]^-$, $[FeCl_4]^-$ and $[FeBr_4]^-$, respectively. In all four complexes, each metal atom has an octahedral geometry as the SHAPE[33] calculation shows (Table S2). The basal plane of the three Fe atoms in the five compounds is formed by four oxygen atoms from four $RCOO^-$ ligands (the Fe-O bond distances range from 1.997(4) to 2.042(4) Å). One apical ligand corresponds to the central μ_3-O (O1) with Fe-O1 bond distances between 1.8987(7) and 1.969(4) Å, while an oxygen atom (O31) of the acetamide ligand occupies the other axial position (Figure 1).

For **1-BF$_4$** the Fe-Fe distances in the triangular unit are all different: 3.308(1), 3.287(1) and 3.297(1) Å, giving rise to a scalene triangle. In **1-GaCl$_4$,** **1-FeCl$_4$** and **1-FeBr$_4$** the cations have C_3 symmetry and, therefore, the three iron centers are crystallographically equivalent, with metal-metal distances of 3.313(1), 3.289(1) and 3.309(1) Å, respectively. In all three compounds the equilateral triangles are eclipsed along the C_3 axis. Interestingly, the equilateral arrangement has only been reported in a few cases, since in most triangular $[Fe_3O]^+$ clusters the Fe centers form isosceles or scalene triangles (Table S3). [22–24,34] An interesting example of equilateral triangle is compound $[Fe_3O(ClCH_2COO)_6(H_2O)_3]ClO_4{\cdot}9H_2O$[35] (CCDC code **SEFHAO**) since it crystallizes in the *R3* space group, as compounds **1-GaCl$_4$,** **1-FeCl$_4$** and **1-FeBr$_4$**. It has been suggested that the equilateral arrangement could be in fact an average structure of different isosceles and/or scalene triangular motifs, however, structural data reported by Boudalis et al.[36] indicate that the equilateral arrangement is maintained even at low temperature with no loss of symmetry.

Interestingly, the disposition of the acetamide ligands causes that the complexes **1-MX$_4$** crystallize in a chiral space group, *R3*. For **1-FeCl$_4$**, the three-acetamide ligands point in the same direction (clockwise), forming an angle of 43.1° between the $[Fe_3O]^+$ plane and the acetamide; this disposition being repeated along the crystal lattice (Figure 2). For **1-FeBr$_4$**, all three acetamide ligands are practically perpendicular to the plane formed by the $[Fe_3O]^+$ unit with an angle of 88.5° (Figure 2). For **1-GaCl$_4$**, the acetamide is partially located in two different positions, with angles of 83.9° and 40.9°, which are quite like those observed for **1-FeCl$_4$** and **1-FeBr$_4$**. Structure **1-BF$_4$** shows that the acetamide ligands point in different directions, that is, two ligands are in a counterclockwise disposition and the third one is clockwise (Figure 1a).

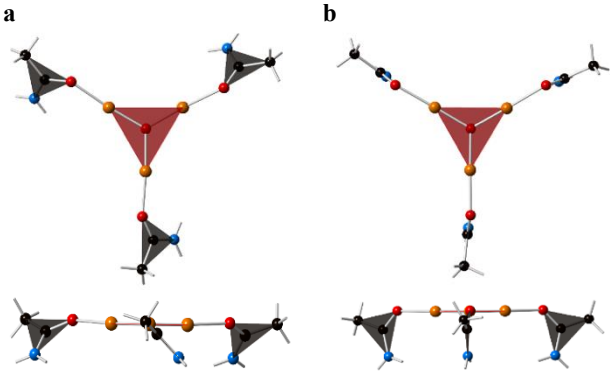

Figure 2. Scheme showing the structural arrangement of the acetamide ligands for **1-FeCl$_4$** (**a**) and **1-FeBr$_4$** (**b**).

The crystal structures of **1-GaCl$_4$,** **1-FeCl$_4$** and **1-FeBr$_4$** aligned symmetrically through the *c axis*. This arrangement is similarly to the one observed for the $[Fe_3O(Ac)_6(H_2O)_3][ClO_4]{\cdot}$(py), in which the triangular units are aligned along the *c axis* (CCDC code **QOPLUC**).[4] For **1-BF$_4$** no order of the triangular units along any of the crystallographic axis is observed. The crystal structures of **1-MX$_4$** are completed by the presence of tetrahedral $[MX_4]^-$ anions (M = Fe^{III} and Ga^{III}), located on the crystallographic 3-fold axis, which passes through one of the M-X bonds. These anions lie symmetrically between the $[Fe_3O(Ac)_6(AcNH_2)_3]^+$ units, thus generating an arrangement that propagates along the *c* axis with M(anion)-Fe(cation) distances of 6.9387(14) and 6.4766(14) Å for **1-GaCl$_4$**, 6.8419(24) and 6.5973(24) Å for **1-FeCl$_4$** and 7.0946(20) and 6.3889(20) Å for **1-FeBr$_4$**. The distance between the M^{III} atoms of neighboring $[MCl_4]^-$ units along the chain is 9.9936(8), 9.8612(14) and 10.1876(14) Å for **1-GaCl$_4$**, **1-FeCl$_4$** and **1-FeBr$_4$**, respectively. It is important to note that very few M_3O clusters with $[MX_4]^-$ anions have been reported.[37–44]

Magnetic Properties

dc Magnetic measurements

The $\chi T(T)$ curve depicted in Figure 3 shows the existence of bulk antiferromagnetic interactions between the Fe^{III} atoms of the $[Fe_3O]^+$ core for all compounds. The χT values at 300 K are 3.45, 4.52, 8.47 and 8.18 emu K mol^{-1} for **1-BF$_4$**, **1-GaCl$_4$,** **1-FeCl$_4$** and **1-FeBr$_4$**, respectively. These values are below the expected ones for four uncoupled high spin paramagnetic Fe^{III} centers present in **1-FeCl$_4$** and **1-FeBr$_4$** and for three uncoupled paramagnetic iron(III) centers in **1-BF$_4$** and **1-GaCl$_4$,** (the expected χT values are, respectively, 17.5 and 13.125 emu mol^{-1} K for g = 2.0). For the compounds with four Fe^{III} centers (**1-FeCl$_4$** and **1-FeBr$_4$**), the χT values decrease continuously until a change in the slope of the curve is observed for the two compounds between ca. 4.3 and 4.6 emu K mol^{-1} that can associated to the trinuclear unit with a S = 1/2 ground state,[45–47] together with the corresponding contribution of the paramagnetic $[FeX_4]^-$ anion (S = 5/2). However, the χT values for the two compounds continues to drop and reaches a value close to 4.0 emu K mol^{-1} at 2 K. For the compounds with three Fe^{III} centers (**1-BF$_4$** and **1-GaCl$_4$**), the susceptibility values decrease reaching values of 0.35 and 0.15 emu mol^{-1} K at 2 K, respectively (Figure 3).

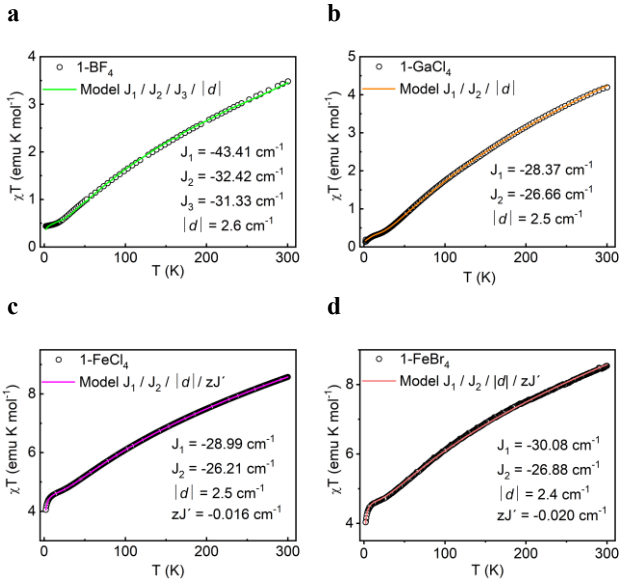

Figure 3. Thermal dependence of χT(T) for compounds **1-BF$_4$**, **1-GaCl$_4$**, **1-FeCl$_4$** and **1-FeBr$_4$** at 1000 G between 2 to 300 K, also showing the curve and values of the best fit parameters obtained considering an isosceles triangle, the antisymmetric exchange, and intermolecular magnetic interactions, see equation S1 and S2.

When the χT value associated to the paramagnetic anion (4.375 emu K mol^{-1}) is subtracted to the experimental value of χ_MT of **1-FeCl$_4$**, a good overlap between this curve and the experimental χ_MT curve of **1-GaCl$_4$** is achieved, except in the low temperature range (Figure 4a). A drop in the χT data for both systems in the temperature range between 2 to 15 K is evident because of the existence of spin-frustration in these systems. Since both systems are iso-structural and therefore should have similar values for the exchange interaction and the antisymmetric exchange, the differences in the χT curves for **1-FeCl$_4$** and **1-GaCl$_4$** at low temperatures, can be considered as due to the intermolecular magnetic interactions between the $[Fe_3O]^+$ and the $[FeX_4^-]$ units along the *c axis*, suggesting that the paramagnetic anion has an effect on the overall magnetic properties (Figure 4a). Moreover, if we subtract the contribution of the paramagnetic anion to the χT curves for **1-FeCl$_4$** and **1-FeBr$_4$** and then compared to the χT values of **1-GaCl$_4$** and for **1-BF$_4$**, it is possible to observe that the susceptibility values at room temperature show differences depending on whether the triangular units are ordered or not. When the triangular units are not ordered, the χT value is lower compared to those compounds where the units are ordered, as can be observed for **1-FeX$_4$** and for **QOPLUC** (Table 2). This difference could be also attributed to the geometry distortions that the local coordination environment may have that could have an effect the overall magnetic properties. In this sense, several discussions have arisen from this point and according to Niedner-Schatteburg et al., spin frustration leads to distortion, but more studies are necessary to understand fully the magnetic properties of frustrated triangular systems.[48–50]

Table 2. Susceptibility values at room temperature for **1-BF$_4$**, **1-GaCl$_4$**, **1-FeCl$_4$**, **1-FeBr$_4$** and **QOPLUC**. T = triangular units, M = Anionic Monomer, S = Solvent Molecule. *Room temperature χ_MT values subtracting the paramagnetic contribution (4.375 emu K mol^{-1}). T = triangular unit and M = monomeric unit.

Complex	χ_MT (300K)	Crystalline Ordering
1-BF$_4$	3.2	Non-ordered triangular units
1-GaCl$_4$	4.2	T-M-T-M-T-M-T… along c axis
1-FeCl$_4$	4.3*	T-M-T-M-T-M-T… along c axis
1-FeBr$_4$	4.4*	T-M-T-M-T-M-T… along c axis
QOPLUC	5	T-S-T-S-T-S-T… along c axis

If we compare the χT value of **1-GaCl$_4$** (crystallographically ordered system) and **1-BF$_4$** (crystallographically non-ordered system), both formed by the same $[Fe_3O]^+$ units and by diamagnetic anions, we can observe differences that can be attributed to electrostatic interactions between the charged species in **1-GaCl$_4$**, meaning that the ordering of these triangular units together with the $[GaCl_4]^-$ units has an effect on the magnetic properties (Figure 4b). Finally, when the anionic unit is intercalated between the triangular cations, the χT value at room temperature is larger than for the non-ordered system, but smaller compared to the ordered and isolated triangular systems, like in **QOPLUC** (Table 2).

For **1-FeCl$_4$** and **1-FeBr$_4$** the behavior of the magnetic susceptibility for cooling and heating cycles becomes completely irreversible in the temperature range 5-15 K. It is worth noting that the susceptibility data show a plateau in the heating up regime, whereas the data do not show this feature for the cooling down regime. This anomalous behavior could be ascribed to the existence of magnetic ordering,[51] but other related magnetic phenomena could be related to this behavior, such as metamagnetism, but further studies are necessary to fully understand and corroborate these observations. However, for **1-GaCl$_4$** the thermal hysteresis is not observed, suggesting that the triangular

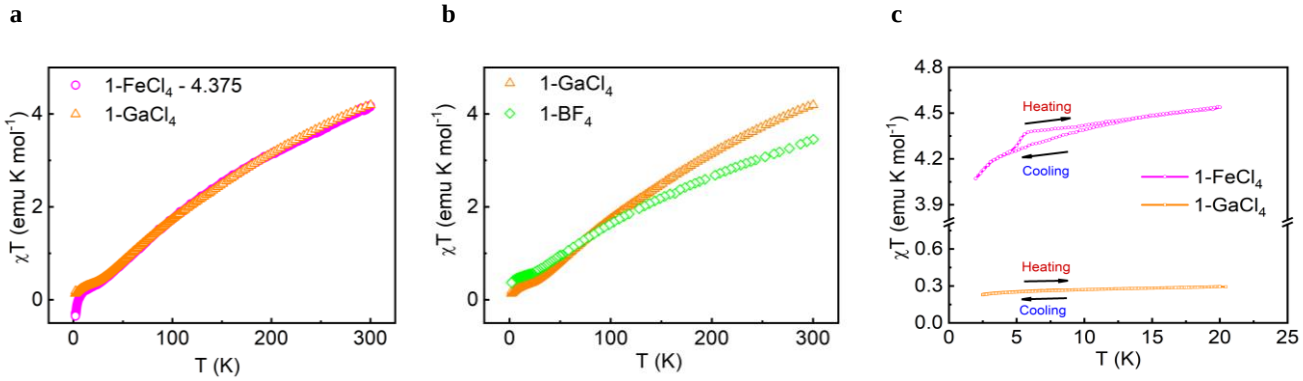

Figure 4. **a**. Comparison between the χ_MT curves of **1-FeCl$_4$** (minus the paramagnetic anion) and **1-GaCl$_4$**. **b**. Comparison between the χ_MT curves of **1-GaCl$_4$** and **1-BF$_4$**. **a** and **c** permit to observe how the magnetic properties of the system can be affected by changing the anion and/or the order of the species in the crystal lattice. **c**. cooling and heating regimes for the magnetic susceptibility data for **1-FeCl$_4$** and **1-GaCl$_4$** at 1000 G.

and paramagnetic units may couple, causing the appearance of these phenomena (Figure 4c and Section S4.1).

The fit of the *dc* experimental data was done using the PHI program.[52] At first only the isotropic interactions for all the triangular arrangements were considered, giving a good fit in the range 20-300 K. The best fit in the all temperature range was achieved by adding to the model, non-isotropic interactions, being these the antisymmetric exchange (ASE; d_{ij}) and the intermolecular interaction (zJ').[36,53–55] For more details, see Section S4.2 in the ESI.

The best fit parameters are listed in Table 3 and the fits are shown as solid lines in Figure 3. The obtained *J* values are within the range observed for other iron(III) oxido-centered carboxylate compounds (see Section S4.3). As can be seen in Table 3, the exchange interactions are different depending on whether the triangular $[Fe_3O]^+$ units are ordered or not in the crystal lattice. The results show that when the triangular units are not ordered (as in **1-BF$_4$**), the overall antiferromagnetic interaction becomes stronger. For the systems ordered along the *c axis* and having $[MX_4]^-$ units intercalated between the triangular units (**1-GaCl$_4$**, **1-FeCl$_4$** and **1-FeBr$_4$**), the exchange interactions are similar between each other. These values are in between those of the non-ordered triangles (**1-BF$_4$**) and ordered triangles with no intercalated $[MX_4]^-$ units like in **QOPLUC**. Table 3 also shows that for the two compounds with paramagnetic $[MX_4]^-$ units (**1-FeCl$_4$** and **1-FeBr$_4$**) the fit of the magnetic properties requires the inclusion of a weak intermolecular magnetic interaction (zJ'), since, otherwise, it is not possible to correctly describe the magnetic properties.

DFT calculations using an approximated model confirm these results and show values of the magnetic interaction between the $[Fe_3O]^+$ fragments and the paramagnetic anions in the range 0.01-0.05 cm^{-1}. These results clearly show that the paramagnetic units are not innocent and influence the *dc* magnetic properties, see Section S4.4 in ESI.

As described in the fitting procedure, the isosceles triangle model with the incorporation of the antisymmetric exchange (which splits the two initially degenerated states), together with the aforementioned weak intermolecular interactions, are necessary to fully describe the susceptibility measurements. This clearly suggests that the anisotropic magnetic interactions affect the magnetic behavior at low temperatures in the studied systems.[5,20] The $|d|$ values obtained for our compounds (in the range 2.4-2.8 cm^{-1}) are slightly larger than those reported by Boudalis *et al*.[36] for **QOPLUC** (1.7 cm^{-1}). Nevertheless, as indicated by this author, higher values of $|d|$ reproduce better the low temperature data of **QOPLUC** but give worse results in the high temperature region due to the small *J* value obtained for **QOPLUC** and the correlation of *J* with $|d|$. In our compounds we have evaluated initially the exchange interactions and then fixed them for the fitting of the low temperature range considering only zJ' and $|d|$. In this way, it is possible to avoid the obtaining of unrealistically small *J* value. Moreover, larger $|d|$ values (up to 5 cm^{-1}) have been reported for $[Fe_3O]^+$ systems, so our results are in the range of previously reported values of other oxo-centered Fe^{III} compounds[53]. As we will show below, this $|d|$ parameter is important in determining the dynamic properties of our triangular Fe^{III} systems.

Table 3. Magnetic *dc* susceptibility best-fit values for the parameters of the best models in the temperature range 2-300 K at 1000 G. Values in cm^{-1}.

Compounds	J_1	J_2	J_3	$\|d\|$	$zJ`$
1-FeCl$_4$	-28.99	-26.21	-	2.5	-0.016
1-FeBr$_4$	-30.08	-26.88	-	2.4	-0.020
1-GaCl$_4$	-28.37	-26.66	-	2.5	-
1-BF$_4$	-32.42	-31.33	-43.41	2.6	
QOPLUC	-22.9	-19.1	-	1.7	-

The field dependence of the reduced magnetization at 2 K for all compounds is shown in Section S4.5 in ESI. At 5 T the magnetization values correspond to *ca*. 0.7, 0.8, 5.5 and 5.6 electrons for **1-BF$_4$**, **1-GaCl$_4$, 1-FeCl$_4$** and **1-FeBr$_4$**, respectively (Figure S8). Literature reports that these systems with a μ_3-oxido moiety show a ground state of S = 1/2 (Nβ = 1),[46,47] although usually these systems present magnetization values below the expected ones, and do not reach saturation even at high fields.[55–57] Comparison of the experimental data with those calculated by the simulation with the program PHI for the four compounds shows a good agreement between them. The lower values of the experimental data confirm the presence of antisymmetric exchange and/or intermolecular interactions.

ac Magnetic measurements

The *ac* susceptibility measurements were carried out for the four compounds: **1-BF$_4$**, **1-GaCl$_4$**, **1-FeCl$_4$** and **1-FeBr$_4$**, see section S5 in ESI. When no *dc* field is applied, none of them shows an out-of-phase signal, χ". Compound **1-BF4** shows no *ac* signal at any frequency under different *dc* fields (Figure 4a and S9). Compound **1-GaCl$_4$** shows a weak out-phase signal, under an applied *dc* field, at high frequencies and low temperatures, indicating the presence of slow relaxation of the magnetization due to the magnetic uniaxial anisotropy in this system (Figure 4b and S10). When *dc* fields of 3000, 5000 and 7000 G are applied, frequency-dependent signals are observed for the two compounds with paramagnetic $[MX_4]^-$ anions: **1-FeCl$_4$** and **1-FeBr$_4$**. No clear maxima can be observed when $\chi``(\upsilon)$ is plotted (Figure S11). For $\chi``$(T) at frequencies above 1000 Hz, under 3000 G, clear maxima can be observed at low temperatures, although at lower frequencies no maxima are detected for **1-FeCl$_4$** and **1-FeBr$_4$** (Figure 4c and 4d).

Boudalis *et al*.[58], studied the dynamic magnetic properties on highly ordered (along the *c* axis) and well isolated (by benzene rings) triangular Fe^{III} S = 1/2 systems. As mentioned above, the ordered compounds **1-GaCl$_4$**, **1-FeCl$_4$** and **1-FeBr$_4$** also present dynamic magnetic properties, in contrast to compound **1-BF$_4$** that also has a S = 1/2 ground state but has no order along any axis and does not present slow relaxation of the magnetization. These results suggest that the ordering of the triangular units, together with the disposition of the diamagnetic and paramagnetic anions influences the dynamic magnetic properties.

a

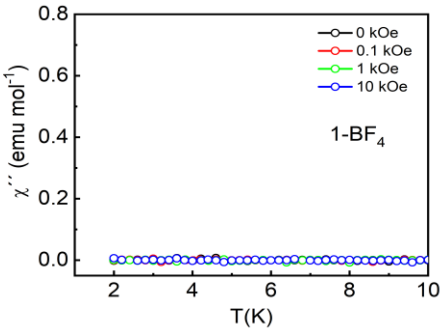

b

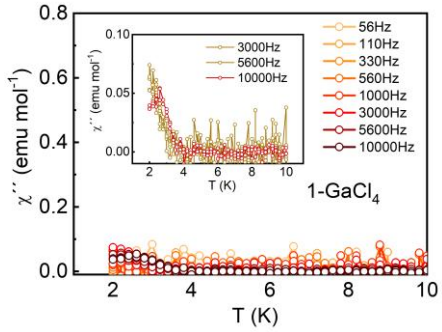

c

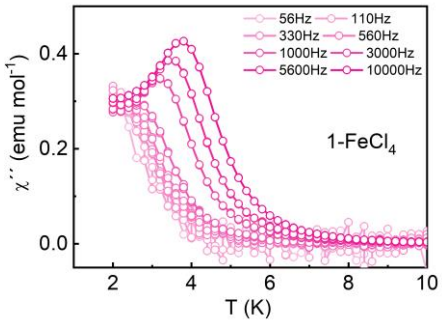

d

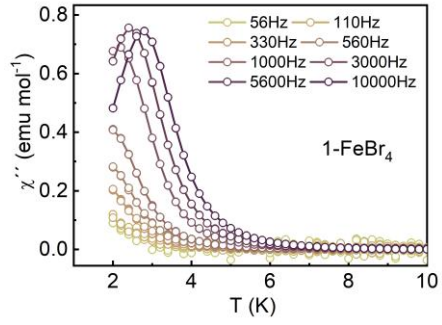

Figure 4. Thermal variation of the out-of-phase susceptibility at different frequencies under a H_{dc} = 3000 G for **1-FeCl₄** (a), **2-GaCl₄** (b), **2-FeCl₄** (c) and **2-FeBr₄** (d).

The dynamic relaxation of these systems shows a complex temperature dependence since, besides the Orbach mechanism for the relaxation, phonon type relaxation mechanism can exist. Then, the relaxation dynamics can be defined as:

$$\tau^{-1} = \tau_{Orbach} + \tau_{Raman}$$

$$\tau^{-1} = \tau_0 e^{U_{eff}/k_B T} + CT^n$$

The Orbach mechanism involves a relaxation through the S = 1/2 ground state to the second S = 1/2 state since the systems are not degenerated. The energy differences between each state are denoted as Δ, equivalent to the energy barrier of the relaxation of the magnetization (U_{eff}). In order to quantify the magnitude of Δ, we have consider the approximation defined by Ferrer et al.[59] for a triangular systems having S = 5/2 centers, in which the parameter Δ can be evaluated from the J_i and $|d|$ values obtained from the susceptibility data:

$$U_{eff} \approx \Delta = (9(J_1 - J_2)^2 + 243|d|)^{1/2}$$

With this equation, the Δ (U_{eff}) values calculated for **1-FeCl₄** and **1-FeBr₄** are 26.0 and 25.9 cm^{-1}, respectively. The fitting procedure consider the Δ (U_{eff}) values as a fix parameter, and only the τ_0, n, C are the fitting variables (Table 4). The obtained values reproduce satisfactorily the dynamic magnetic properties of compounds **1-FeCl₄** and **1-FeBr₄** (Figure 5), confirming the validity of the *J* and $|d|$ values obtained from *dc* magnetic measurements.

Table 4. Summary of the relaxation parameters obtain under applied *dc* fields for **1-FeCl₄**, **1-FeBr₄** and **QOPLUC**.

Compound	H_{dc} (G)	Δ (cm^{-1})	τ_0 (s) x 10^{-10}	C ($s^{-1}K^{-n}$)	n
1-FeCl₄	3000	26.0	2.2(5)	6.4	5.3
1-FeBr₄	3000	25.9	3.3(8)	36.1	5.5
QOPLUC	750	23	2.0(7)	2700	3.3

The obtained τ_0 values are within the range observed for other compounds with slow relaxation of the magnetization.[60–62] Besides the Orbach mechanism, the relaxation times also follow a phonon type relaxation mechanism (Raman term). The differences in the Raman contributions (C and n values) observed in the two compounds (**1-FeCl₄** and **1-FeBr₄**) can be attributed to the differences in the heteroatom (X = Cl and Br) of the $[MX_4]^-$ anions. The n values of the Raman relaxation obtained in the fit (in the range 5.3-5.5) are lower than the expected ones (n = 9 for Kramer ions). This difference may be attributed to the involvement of both optical and acoustic Raman processes during the magnetic relaxation.[63] We can conclude, therefore, that Orbach and Raman mechanism describe the relaxation dynamics in these compounds, as has been previously reported for other triangular $[Fe_3O]^+$ systems. Finally, the differences in the n and C parameters between compounds **1-FeCl₄** and **1-FeBr₄** and **QOPLUC**, may be related to the presence of paramagnetic anions intercalated between the triangular units in **1-FeCl₄** and **1-FeBr₄** and/or to the disposition of the triangular units and the anions in the crystal lattice. These results confirm the idea that the ordering of the triangular $[Fe_3O]^+$ units and the nature and disposition of the tetrahedral units affect the magnetic properties of triangular Fe^{III} S = 1/2 systems. Finally, Cole-Cole plots show an alpha value of 0.22 for **1-FeCl₄**, which is relatively large, thus suggesting that more than one relaxation mechanism exists, in this sense, the Orbach and Raman ones, as describe above (Figure S15).

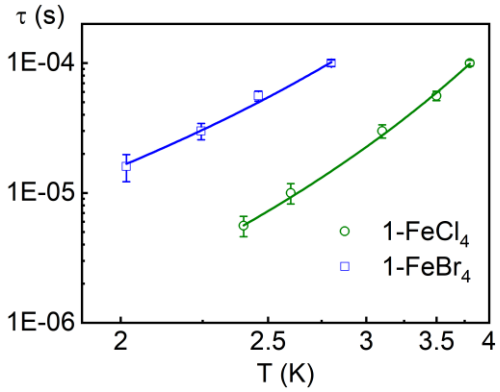

Figure 5. Temperature dependence of the relaxation time τ for **1-FeCl$_4$** (green) and **1-FeBr$_4$** (blue) under an H_{dc} = 3000 G. The experimental data are shown as open shapes, and the solid line corresponds to the best fit.

CONCLUSIONS

Four new trinuclear $[Fe_3O]^+$ complexes with paramagnetic and diamagnetic tetrahedral anions have been obtained $[Fe_3O(Ac)_6(AcNH_2)_3][BF_4]\cdot(CH_3CONH_2)_{0.5}(H_2O)_{0.5}$ (**1-BF$_4$**), $[Fe_3O(Ac)_6(AcNH_2)_3][GaCl_4]$ (**1-GaCl$_4$**), $[Fe_3O(Ac)_6(AcNH_2)_3][FeCl_4]$ (**1-FeCl$_4$**) and $[Fe_3O(Ac)_6(AcNH_2)_3][FeBr_4]$ (**1-FeBr$_4$**).

The three compounds with $[MX_4]^-$ anions, M = Fe^{III} and Ga^{III}, form highly ordered systems along a crystallographic axis. The *dc* magnetic properties reflect that the paramagnetic or diamagnetic nature of the anions, as well as the ordering of the triangular units in the crystal lattice have an effect on the bulk magnetic properties of the systems. The *ac* susceptibility data show that all the complexes with paramagnetic tetrahalogenometalate anions (**1-FeCl$_4$**, **1-GaCl$_4$** and **1-FeBr$_4$**) present slow relaxation of the magnetization.

The relaxation dynamics analysis of these systems suggests that phonon type mechanism seems to be affecting the relaxation dynamics of these systems, together with the Orbach type mechanism. The ordering of the triangular Fe^{III} S = 1/2 units and the paramagnetic anions in the crystal lattice influence the phonon relaxation mechanism.

ASSOCIATED CONTENT

Supporting Information.

The Supporting Information is available free of charge at https://pubs.acs.org/doi/10.1021/acs.cgd.XXXXX.

Experimental details related to the FTIR, ESI-MS, structural analysis, *dc* magnetic measurements with DFT calculations and *ac* magnetic measurements are presented (PDF).

Access CCDC Codes

CCDC 1547609 **(1-BF$_4$)**, 1547610 **(1-GaCl$_4$)**, CCDC-1547607 **(1-FeCl$_4$)** and 1547608 **(1-FeBr$_4$)** contain the supplementary crystallographic data for this paper. These data can be obtained free of charge via www.ccdc.cam.ac.uk/data_request/cif, or by emailing data_request@ccdc.cam.ac.uk, or by contacting The Cambridge Crystallographic Data Centre, 12 Union Road, Cambridge CB2 1EZ, UK; fax: +44 1223 336033.

ACKNOWLEDGEMENTS

Authors acknowledge Financiamiento Basal Program AFB180001 and Anillo ACT-1404 (IPMaG) for partial financial support. Powered@NLHPC: This research was partially supported by the supercomputing infrastructure of the NLHPC (ECM-02), Centre for Mathematical Modelling CMM, Universidad de Chile. The authors thank Quantum Design Inc. for the measurements done using a PPMS® DynaCool™. The authors acknowledge CONICYT-FONDEQUIP/EQM130086-EQM140060. This work was done under the LIA-M3-1027 CNRS Collaborative Program. The present work has been funded by the Spanish MINECO grant CTQ-2017-87201-P-AEI/FEDER, EU and 'Unidad de Excelencia María de Maeztu' MDM-2015-0538 granted to ICMol, and the Generalidad Valenciana (Prometeo/2019/076 program of excellence). G.M.E acknowledges funding from the MINECO (Ramón y Cajal contract).

AUTHOR INFORMATION

ORCID

Walter Cañón-Mancisidor: orcid.org/0000-0003-1703-8729
Diego Venegas-Yazigi: orcid.org/0000-0001-7816-2841
Evgenia Spodine: orcid.org/0000-0002-7089-3145
Patricio Hermosilla-Ibáñez: orcid.org/0000-0002-2272-9690
Verónica Paredes-García: orcid.org/0000-0002-7537-7430
Carlos J. Gómez-García: orcid.org/0000-0002-0015-577X.
Guillermo Mínguez Espallargas: orcid.org/0000-0001-7855-1003.

Notes

The authors declare no competing financial interest.

 # = Dedicated to our distinguished colleague and friend Dr. Jean-René Hamon on the occasion of his 65th birthday.

REFERENCES

(1) Trif, M.; Troiani, F.; Stepanenko, D.; Loss, D. Spin-Electric Coupling in Molecular Magnets. *Phys. Rev. Lett.* **2008**, *101*, 1–4.

(2) Troiani, F.; Stepanenko, D.; Loss, D. Hyperfine-Induced Decoherence in Triangular Spin-Cluster Qubits. *Phys. Rev. B - Condens. Matter Mater. Phys.* **2012**, *86*, 161409.

(3) Spielberg, E. T.; Gilb, A.; Plaul, D.; Geibig, D.; Hornig, D.; Schuch, D.; Buchholz, A.; Ardavan, A.; Plass, W. A Spin-Frustrated Trinuclear Copper Complex Based on Triaminoguanidine with an Energetically Well-Separated Degenerate Ground State. *Inorg. Chem.* **2015**, *54*, 3432–3438.

(4) Sowrey, F. E.; Tilford, C.; Wocadlo, S.; Anson, C. E.; Powell, A. K.; Bennington, S. M.; Montfrooij, W.; Jayasooriya, U. A.; Cannon, R. D. Spin Frustration and Concealed Asymmetry: Structure and Magnetic Spectrum of $[Fe_3O(O_2CPh)_6(Py)_3]ClO_4\cdot py$†. *J. Chem. Soc. Dalt. Trans.* **2001**, *6*, 862–866.

(5) Tsukerblat, B.S.; Belinskii, M.I.; Fainzil´berg, V. E. Magnetochemistry and Spectroscopy of Transition Metals Exchange Clusters. *Sov. Sci. Rev. B Chem.* **1987**, *9*, 337–481.

(6) Earnshaw, A.; Figgis, B. N.; Lewis, J. Chemistry of Polynuclear Compounds. Part VI. Magnetic Properties of Trimeric Chromium and Iron Carboxilates. *J. Chem. Soc.* **1966**, 1656–1663.

(7) Duncan, J. F.; Kanekar, C. R.; Mok, K. F. Some Trinuclear Iron(III) Carboxylate Complexes. *J. Chem. Soc.* **1969**, 480–482.

(8) Cannon, R. D.; White, R. P. Chemical and Physical Properties of Triangular Bridged Metal Complexes. *Prog. Inorg. Chem.* **1988**, *36*, 195–298.

(9) Cannon, R. D.; Jayasooriya, U. A.; Wu, R.; Koske, S. K.; Stride, J. A.; Nielsen, O. F.; White, R. P.; Kearley, G. J.; Summerfield, D. Spin Frustration in High-Spin Triiron (III) Complexes: An Inelastic Neutron Scattering Study. *J. Am. Chem. Soc.* **1994**, *116*, 11869–11874.

(10) Wu, R.; Poyraz, M.; Sowrey, F. E.; Anson, C. E.; Wocadlo, S.; Powell, A. K.; Jayasooriya, U. A.; Cannon, R. D.; Nakamoto, T.; Katada, M.; Sano, H.; Women, O. Electron Localization and Delocalization in Mixed-Valence Transition Metal Clusters : Structural and Spectroscopic Studies of Oxo-Centered Trinuclear Complexes. *Inorg. Chem.* **1998**, *37*, 1913–1921.

(11) Vincent, J. B.; Chang, H. R.; Folting, K.; Huffman, J. C.; Christou, G.; Hendrickson, D. N. Preparation and Physical Properties of Trinuclear Oxo-Centered Manganese Complexes of General Formulation $[Mn_3O(O_2CR)_6L_3]^{0,+}$ (R = Methyl or Phenyl; L = a Neutral Donor Group) and the Crystal Structures of $[Mn_3O(O_2CMe)_6(Pyr)_3](Pyr)$ and $[Mn_3O(O_2CPh)_6(Pyr)_2(H_2O)]\cdot cntdot\cdot 0.5MeCN$. *J. Am. Chem. Soc.* **1987**, *109*, 5703–5711.

(12) Gorun, S. .; Papaefthymiou, G. C.; Frankel, R. B.; Lippard, S. J. Synthesis, Structure, and Magnetic and Moessbauer Properties of Mononuclear and Asymmetric, Oxo-Bridged Trinuclear Iron (III) Complexes of a New Polyimidazole. *J. Am. Chem. Soc.* **1987**, *109*, 4244–4255.

(13) McCusker, J. K.; Jang, H. G.; Wang, S.; Christou, G.; Hendrickson, D. N. Ground-State Variability in μ_3-Oxide Trinuclear Mixed-Valence Manganese Complexes: Spin Frustration. *Inorg. Chem.* **1992**, *31*, 1874–1880.

(14) Vlachos, A.; Psycharis, V.; Raptopoulou, C. P.; Lalioti, N.; Sanakis, Y.; Diamantopoulos, G.; Fardis, M.; Karayanni, M.; Papavassiliou, G.; Terzis, A. A Nearly Symmetric Trinuclear Chromium(III) Oxo Carboxylate Assembly: Preparation, Molecular and Crystal Structure, and Magnetic Properties of $[Cr_3O(O_2CPh)_6(MeOH)_3](NO_3)\cdot 2MeOH$. *Inorg. Chim. Acta* **2004**, *357*, 3162–3172.

(15) Tong, M.; Chen, X.; Sun, Z.-M.; Hendrickson, D. N. Synthesis , Crystal Structure and Magnetic Properties of Triaquahexakis-(μ_2-Betaine)(μ_3-Oxo)Triiron(III) Perchlorate Heptahydrate. *Transit. Met. Chem.* **2001**, *26*, 195–197.

(16) Catterick, J.; Thornton, P.; Fitzsimmons, B. W. Synthesis, Magnetic Properties and Mossbauer Spectra of Polynuclear Iron Carboxilates. *J. Chem. Soc. Dalt. Trans.* **1977**, 1420–1425.

(17) Psycharis, V.; Raptopoulou, C. P.; Boudalis, A. K.; Sanakis, Y.; Fardis, M.; Diamantopoulos, G.; Papavassiliou, G. Syntheses, Structural, and Physical Studies of Basic Cr^{III} and Fe^{III} Benzilates and Benzoates: Evidence of Antisymmetric Exchange and Distributions of Isotropic and Antisymmetric Exchange Parameters. *Eur. J. Inorg. Chem.* **2006**, *2006*, 3710–3723.

(18) Dendrinou-Samara, C.; Katsamakas, S.; Raptopoulou, C.; Terzis, A.; Tangoulis, V.; Kessissoglou, D. P. Interaction of Fe(III) with Herbicide-Carboxylato Ligands - Di-, Tri- and Tetra-Nuclear Compounds: Structure and Magnetic Behavior. *Polyhedron* **2007**, *26*, 763–772.

(19) Robert, J.; Parizel, N.; Turek, P.; Boudalis, A. K. Relevance of Dzyaloshinskii–Moriya Spectral Broadenings in Promoting Spin Decoherence: A Comparative Pulsed-EPR Study of Two Structurally Related Iron(III) and Chromium(III) Spin-Triangle Molecular Qubits. *Phys. Chem. Chem. Phys.* **2019**, *21* (35), 19575–19584.

(20) Boudalis, A. K. Half-Integer Spin Triangles: Old Dogs, New Tricks. *Chem. – A Eur. J.* **2021**, *27*, 7022–7042.

(21) Mitrikas, G.; Sanakis, Y.; Raptopoulou, C. P.; Kordas, G.; Papavassiliou, G. Electron Spin-Lattice and Spin-Spin Relaxation Study of a Trinuclear Iron(III) Complex and Its Relevance in Quantum Computing. *Phys. Chem. Chem. Phys.* **2008**, *10*, 743–748.

(22) Thundathil, R. V; Holt, E. M.; Watsodb, K. J.; Halt, S. L. Preparation and Properties of Iron(III)-Amino Acid Complexes. 2 . The Crystal and Molecular Structure of Monoclinic Tri-μ_3-oxo-Triaquohexakis(glycine)triiron (III) Perchlorate. *J. Am. Chem. Soc.* **1977**, *99*, 1818–1823.

(23) Degang, F.; Guoxiong, W.; Wenxia, T. The Structure and Magnetic Properties of μ_3-oxotriiron(III) Complex $[Fe_3O(OBZ)_6(CH_3OH)_3](NO_3)(CH_3OH)_2$ (HOBZ = Benzoic Acid). *Polyhedron* **1993**, *12*, 2459–2463.

(24) Bond, A. M.; Clark, R. J. H.; Humphrey, D. G.; Panayiotopoulos, P.; Skelton, B. W.; White, A. H. Synthesis, characterisation and electrochemical reductions of oxo-centred, carboxylate-bridged triiron complexes, $[Fe_3(\mu_3\text{-}O)(\mu\text{-}O_2CR)_6L_3]X$ (R = Me, But, Ph, CH_2Cl, CCl_3, CH_2CN or 4-$NO_2C_6H_4$; L = Py, 3-H_2Npy, 4-H_2Npy, 3-NCpy, 4-NCpy or 4-CH_2CHpy; X = ClO_4^- or NO_3^-). *J. Chem. Soc. Dalt. Trans.* **1998**, 1845–1852.

(25) Blake, A. B.; Fraser, L. R. Crystal Structure and Mass Spectrum of μ_3-Oxo-hexakis(μ-trimethyl- Acetate)-Trismethanoltri-Iron(III) Chloride, a Trinuclear Basic Iron(III) Carboxylate. *J. Chem. Soc. Dalt. Trans.* **1975**, 193–197.

(26) Long, D.-L.; Kögerler, P.; Farrugia, L. J.; Cronin, L. Linking Chiral Clusters with Molybdate Building Blocks: From Homochiral Helical Supramolecular Arrays to Coordination Helices. *Chem. – An Asian J.* **2006**, *1*, 352–357.

(27) SAINTPLUS, 1999, Version 6.02; Brucker AXS: Madison, WI, USA.

(28) Sheldrick, G. M. SHELXT – Integrated Space-Group and Crystal-Structure Determination. *Acta Crystallogr. Sect. A Found. Adv.* **2015**, *71*, 3–8.

(29) Sheldrick, G. M. Crystal Structure Refinement with SHELXL. *Acta Crystallogr. Sect. C Struct. Chem.* **2015**, *71*, 3–8.

(30) K. Brandenburg, Diamond, Version 3.2k, Cryst. Impact GbR, Bonn, Germany, **2014**.

(31) Bain, G. A.; Berry, J. F. Diamagnetic Corrections and Pascal's Constants. *J. Chem. Educ.* **2008**, *85*, 532–536.
(32) Izzo, B.; Klein, M. T.; LaMarca, C.; Scrivner, N. C. Hydrothermal Reaction of Saturated and Unsaturated Nitriles: Reactivity and Reaction Pathway Analysis. *Ind. Eng. Chem. Res.* **1999**, *38*, 1183–1191.
(33) Casanova, D.; Cirera, J.; Llunell, M.; Alemany, P.; Avnir, D.; Alvarez, S. Minimal Distortion Pathways in Polyhedral Rearrangements. *J. Am. Chem. Soc.* **2004**, *126*, 1755–1763.
(34) Hibbs, W.; van Koningsbruggen, P. J.; Arif, A. M.; Shum, W. W.; Miller, J. S. One- and Two-Step Spin-Crossover Behavior of $[Fe^{II}(Isoxazole)_6]^{2+}$ and the Structure and Magnetic Properties of Triangular $[Fe^{III}_3O(OAc)_6(Isoxazole)_3][ClO_4]$. *Inorg. Chem.* **2003**, *42*, 5645–5653.
(35) Dutta, A. K.; Maji, S. K.; Dutta, S. A Symmetric oxo-centered trinuclear chloroacetato bridged iron(III) complex: structural, spectroscopic and electrochemical Studies. *J. Mol. Struct.* **2012**, *1027*, 87–91.
(36) Georgopoulou, A. N.; Margiolaki, I.; Psycharis, V.; Boudalis, A. K. Dynamic versus Static Character of the Magnetic Jahn-Teller Effect: Magnetostructural Studies of $[Fe_3O(O_2CPh)_6(Py)_3]ClO_4$·py. *Inorg. Chem.* **2017**, *56* (2), 762–772.
(37) Shova, S. G.; Cadelnic, I. G.; Gdaniec, M.; Simonov, Y. A.; Jovmir, T. C.; Meriacre, V. M.; Filoti, G.; Turta, C. I. Synthesis and Structural Study of Trinuclear Iron Acetates $[Fe_3O(CH_3COO)_6(H_2O)_3]Cl·6H_2O$ and $[Fe_3O(CH_3COO)_6(H_2O)_3][FeCl_4]·2CH_3COOH$. *J. Struct. Chem.* **1998**, *39*, 747–761.
(38) Sudik, A. C.; Côté, A. P.; Yaghi, O. M. Metal-Organic Frameworks Based on Trigonal Prismatic Building Blocks and the New "Acs" Topology. *Inorg. Chem.* **2005**, *44* (9), 2998–3000.
(39) Fursova, E. Y.; Romanenko, G. V; Ovcharenko, V. I. Hexanuclear methanediolate bridged iron(III) complex. *Russ. Chem. Bull. Int. Ed.* **2005**, *54*, 811–813.
(40) Ogrin, D.; Barron, A. R. Synthesis and Structure of $[Fe_3O(O_2CCH_2OMe)_6(H_2O)_3][FeCl_4]$. *J. Chem. Crystallogr.* **2008**, *39*, 68–72.
(41) Prodius, D.; Macaev, F.; Stingaci, E.; Pogrebnoi, V.; Mereacre, V.; Novitchi, G.; Kostakis, G. E.; Anson, C. E.; Powell, A. K. Catalytic "Triangles": Binding of Iron in Task-Specific Ionic Liquids. *Chem. Commun.* **2013**, *49*, 1915–1917.
(42) Lu, M.; Chen, T.; Wang, M.; Jiang, G.; Lu, T.; Jiang, G.; Du, J. A New μ_3-oxo-centered tri-nuclear carboxyl bridged iron(III) complex with thio-methyl groups in the periphery: structural, spectroscopic and electrochemical Studies. *J. Mol. Struct.* **2014**, *1060*, 131–137.
(43) Marchetti, F.; Melai, B.; Pampaloni, G.; Zacchini, S. Synthesis and Reactivity of Haloacetato Derivatives of Iron (II) Including the Crystal and the Molecular Structure of $[Fe(CF_3COOH)_2(\mu\text{-}CF_3COO)_2]_n$. *Inorg. Chem.* **2007**, *46*, 3378–3384.
(44) Amani, V.; Safari, N.; Khavasi, H. R. Solution and solid state characterization of oxo-centered trinuclear iron(III) Acetate Complexes $[Fe_3(\mu_3\text{-}O)(\mu\text{-}OAc)_6(L)_3]^+$. *Spectrochim. Acta. A. Mol. Biomol. Spectrosc.* **2012**, *85*, 17–24.
(45) Dziobkowski, C. T.; Wrobleski, J. T.; Brown, D. B. Magnetic properties and mössbauer, spectra of several iron(III)-dicarboxylic acid complexes. *Inorg. Chem.* **1981**, *20*, 671–678.
(46) Boudalis, A. K.; Sanakis, Y.; Dahan, F.; Hendrich, M.; Tuchagues, J.-P. An octanuclear complex containing the $[Fe_3O]^{7+}$ metal core: structural, magnetic, mössbauer, and electron paramagnetic resonance studies. *Inorg. Chem.* **2006**, *45*, 443–453.
(47) Boudalis, A. K.; Sanakis, Y.; Raptopoulou, C. P.; Terzis, A.; Tuchagues, J.-P.; Perlepes, S. P. A Trinuclear Cluster Containing the $\{Fe_3(\mu_3\text{-}O)\}^{7+}$ Core: Structural, Magnetic and Spectroscopic (IR, Mössbauer, EPR) Studies. *Polyhedron* **2005**, *24*, 1540–1548.
(48) Lang, J.; Hewer, J. M.; Meyer, J.; Schuchmann, J.; van Wüllen, C.; Niedner-Schatteburg, G. Magnetostructural Correlation in Isolated Trinuclear Iron(III) Oxo Acetate Complexes. *Phys. Chem. Chem. Phys.* **2018**, *20*, 16673–16685.
(49) Antkowiak, M.; Kamieniarz, G.; Florek, W. Comment on "Magnetostructural Correlations in Isolated Trinuclear Iron(III) Oxo Acetate Complexes" by J. Lang, J. M. Hewer, J. Meyer, J. Schuchmann, C. van Wüllen and G. Niedner-Schatteburg, Phys. Chem. Chem. Phys., 2018, 20, 16673. *Phys. Chem. Chem. Phys.* **2019**, *21*, 504.
(50) van Wüllen, C.; Lang, J.; Niedner-Schatteburg, G. Reply to the 'Comment on "Magnetostructural Correlations in Isolated Trinuclear Iron(III) Oxo Acetate Complexes"' by M. Antkowiak, G. Kamieniarz and W. Florek, *Phys. Chem. Chem. Phys.*, 2018, 20, DOI: 10.1039/C8CP04691C. *Phys. Chem. Chem. Phys.* **2019**, *21*, 505–506.
(51) Antonosyan, D.; Bellucci, S.; Ohanyan, V. Exactly Solvable Ising-Heisenberg Chain with Triangular XXZ-Heisenberg Plaquettes. *Phys. Rev. B - Condens. Matter Mater. Phys.* **2009**, *79* (1), 014432.
(52) Chilton, N. F.; Anderson, R. P.; Turner, L. D.; Soncini, A.; Murray, K. S. PHI: A Powerful New Program for the Analysis of Anisotropic Monomeric and Exchange-Coupled Polynuclear d- and f-Block Complexes. *J. Comput. Chem.* **2013**, *34*, 1164–1175.
(53) Piñero, D.; Baran, P.; Boca, R.; Herchel, R.; Klein, M.; Raptis, R. G.; Renz, F.; Sanakis, Y. A Pyrazolate-Supported $Fe_3(\mu_3\text{-}O)$ Core: Structural, Spectroscopic, Electrochemical, and Magnetic Study. *Inorg. Chem.* **2007**, *46*, 10981–10989.
(54) Sameera, W. M. C.; Piñero, D. M.; Herchel, R.; Sanakis, Y.; McGrady, J. E.; Raptis, R. G.; Zueva, E. M. A Combined Experimental and Computational Study of the Magnetic Superexchange within a Triangular (μ_3-O)-Pyrazolato-Fe^{III}_3 Complex. *Eur. J. Inorg. Chem.* **2012**, *2012*, 3500–3506.
(55) Raptopoulou, C. P.; Sanakis, Y.; Boudalis, A. K.; Psycharis, V. Salicylaldoxime (H_2salox) in Iron(III) Carboxylate Chemistry: Synthesis, X-Ray Crystal Structure, Spectroscopic Characterization and Magnetic Behavior of Trinuclear Oxo-Centered Complexes. *Polyhedron* **2005**, *24*, 711–721.
(56) Alborés, P.; Rentschler, E. Structural and Magnetic Characterization of a μ-1,5-Dicyanamide-Bridged Iron Basic Carboxylate $[Fe_3O(O_2C(CH_3)_3)_6]$ 1D Chain. *Inorg. Chem.* **2008**, *47*, 7960–7962.
(57) Francois, M.; Saleh, M. I.; Rabu, P.; Souhassou, M.; Malaman, B.; Steinmetz, J. Structural Transition at 225

K of the Trinuclear Fe(III) Heptanoate $[Fe_3O(O_2CC_6H_{13})_6(H_2O)_3]NO_3$. *Solid State Sci.* **2005**, *7*, 1236–1246.

(58) Georgopoulou, A. N.; Sanakis, Y.; Boudalis, A. K. Magnetic Relaxation in Basic Iron(III) Carboxylate $[Fe_3O(O_2CPh)_6(H_2O)_3]ClO_4 \cdot py$. *Dalton Trans.* **2011**, *40*, 6371–6374.

(59) Ferrer, S.; Lloret, F.; Pardo, E.; Clemente-Juan, J. M.; Liu-González, M.; García-Granda, S. Antisymmetric Exchange in Triangular Tricopper(II) Complexes: Correlation among Structural, Magnetic, and Electron Paramagnetic Resonance Parameters. *Inorg. Chem.* **2012**, *51*, 985–1001.

(60) Sun, H. L.; Wang, Z. M.; Gao, S. Strategies towards Single-Chain Magnets. *Coord. Chem. Rev.* **2010**, *254*, 1081–1100.

(61) Winpenny, R. *Single-Molecule Magnets and Related Phenomena*; Winpenny, R., Ed.; Structure and Bonding; Springer-Verlag: Berlin/Heidelberg, 2006; Vol. 122.

(62) Craig, G. A.; Murrie, M. 3d Single-Ion Magnets. *Chem. Soc. Rev.* **2015**, *44*, 2135–2147.

(63) Shrivastava, K. N. Theory of Spin–Lattice Relaxation. *Phys. Status Solidi* **1983**, *117*, 437–458.

For Table of Contents Use Only

Slow relaxation of the magnetization on frustrated triangular Fe^{III} units with S = 1/2 ground state: the effect of the highly ordered crystal lattice and the counter-anions

Walter Cañón-Mancisidor*, Patricio Hermosilla-Ibáñez, Evgenia Spodine*, Verónica Paredes-García, Carlos J. Gómez-García, Guillermo Mínguez Espallargas, Diego Venegas-Yazigi*.

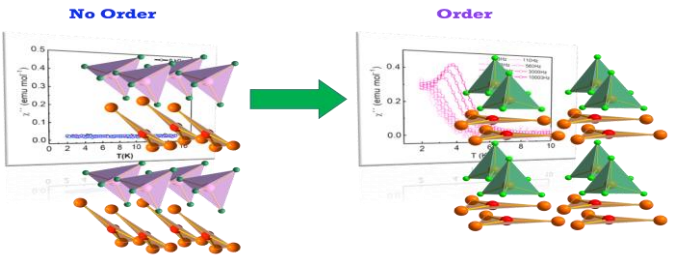

The disposition of the frustrated triangular Fe^{III} units and their counter-anions in the crystal lattice cause a change in the magnetic response, inducing the appearance of slow relaxation of the magnetization.